Table I. Acid Dissociation Constants, Calculated from the Nernst–Clark Plots of Figure 4, for Water Molecules Ligated to the Various Oxidation States of the Chromium 5,10,15,20-Tetrakis-(2,6-dimethyl-3-sulfonatophenyl)porphyrin Species

species	pK_{a1}	pK_{a2}
$(1^{\bullet-})Cr^{II}(H_2O)_2$	10.6 ± 0.3[a,f]	NO[b]
$(1)Cr^{II}(H_2O)_2$	10.6 ± 0.3[c]	NO[b]
$(1)Cr^{III}(H_2O)_2$	9.1 ± 0.3[c]	NO[b]
	9.6 ± 0.3[d]	12.4 ± 0.3[d]
$(1^{\bullet+})Cr^{III}(H_2O)_2$	9.6 ± 0.3[a,d]	12.4 ± 0.3[a,d]
$(1)Cr^{IV}(H_2O)_2$	7.6 ± 0.2[d]	10.2 ± 0.3[d]
	7.5 ± 0.2[e]	NO[b]
$(1)Cr^{V}(H_2O)_2$	7.1 ± 0.2[e]	NO[b]

[a] Acid dissociation constants of the π cation radical and the π anion radical are identical with those of same oxidation states of chromium porphyrins. [b] NO means not observed. [c] Determined from the one-electron reduction of $(1)Cr^{III}(Y)_2$. [d] Determined from the one-electron oxidation of $(1)Cr^{III}(Y)_2$. [e] Determined from the one-electron oxidation of $(1)Cr^{IV}(Y)_2$. [f] Determined from the one-electron reduction of $(1)Cr^{II}(Y)_2$.

metal-centered oxidation to $(1)Cr^{V}(Y)_2$. That $1e^-$ oxidation of $(1)Cr^{IV}(Y)_2$ provides $(1)Cr^{V}(Y)_2$ is, therefore, supported by both the pH dependence of E_m and the observation of the spectrum of $(1)Cr^{V}(Y)_2$ product under the conditions of rapid thin-layer spectroelectrochemical controlled potential oxidation (loc. cit.).

The electrode potential of the first reduction of $(1)Cr^{III}(Y)_2$ shifts from −1.04 V below pH 9 to −1.13 V above pH 10 (Figure 4d). The electrode potential decreases with a slope of about 60 mV/pH between pH 9 and 12. The pH dependence of E_m establishes the reduction as metal-centered to provide $(1)Cr^{II}(Y)_2$. The reversible second reduction of $(1)Cr^{III}(Y)_2$ is pH independent with $E_{1/2}$ at −1.21 V (Figure 4e). This pH independence of E_m shows that the second $1e^-$ reduction may be assigned to the reduction of the porphyrin ring ($(1)Cr^{II}(Y)_2 + 1e^- \rightarrow (1^{\bullet-})Cr^{II}(Y)_2$).

The acid dissociation constants for $(1^{\bullet-})Cr^{II}(Y)_2$, $(1)Cr^{II}(Y)_2$, $(1)Cr^{III}(Y)_2$, $(1)Cr^{IV}(Y)_2$, $(1^{\bullet+})Cr^{III}(Y)_2$, and $(1)Cr^{V}(Y)_2$, which are determined from the fit of the Nernst–Clark plots to the experimental data for the reductions and oxidations of $(1)Cr^{III}(Y)_2$, are provided in Table I.

Of considerable importance is the understanding that H_2O and HO^- are the axial ligands of the chromium porphyrin derivative of various oxidation states in aqueous solutions. The electrochemically measured pK_{a1}^{III} (9.4) and pK_{a2}^{III} (12.4) values for acid dissociation of $(1)Cr^{III}(H_2O)_2$ compare favorably to values determined by spectrophotometric titration (9.0 and 12.6) at an ionic strength of 0.2 M ($NaClO_4$).[4] The decrease of pK_{a1} with an increase in the oxidation state of chromium is reasonable and has precedence[1] in studies with $(1)Fe^{III}(Y)_2$. The pH independence of the electrode potentials in the reductions of chromium(III) porphyrin π cation radical → chromium(III) porphyrin derivative and $(1)Cr^{II}(Y)_2 \rightarrow (1^{\bullet-})Cr^{II}(Y)_2$ is explained on the basis that the electron added to or removed from the porphyrin ring in the course of these reactions is delocalized over the porphyrin 24-atom framework such that the electron density of the Cr^{III} and Cr^{II} water ligation centers are not much altered. Therefore, the pK_a values of the chromium(III) porphyrin π cation radical and $(1^{\bullet-})Cr^{II}(Y)_2$ are almost the same as those of the chromium(III) porphyrin derivative and $(1)Cr^{II}(Y)_2$, respectively.

Acknowledgment. This study was supported by a grant from the National Institutes of Health.

Registry No. $(1)Cr^{II}(H_2O)_2$, 136536-89-5; $(1)Cr^{II}(H_2O)(HO^-)$, 136536-90-8; $(1)Cr^{II}(HO^-)_2$, 136536-91-9; $(1^{\bullet-})Cr^{II}(H_2O)_2$, 136536-92-0; $(1^{\bullet-})Cr^{II}(H_2O)(HO^-)$, 136536-93-1; $(1^{\bullet-})Cr^{II}(HO^-)_2$, 136536-94-2; $(1)Cr^{III}(H_2O)_2$, 136536-95-3; $(1)Cr^{III}(H_2O)(HO^-)$, 136536-96-4; $(1)Cr^{III}(HO^-)_2$, 136536-97-5; $(1)Cr^{IV}(H_2O)_2$, 136536-98-6; $(1)Cr^{IV}(H_2O)(HO^-)$, 136536-99-7; $(1)Cr^{IV}(HO^-)_2$, 136537-00-3; $(1)Cr^{V}(H_2O)_2$, 136537-01-4; $(1)Cr^{V}(H_2O)(HO^-)$, 136545-26-1; $(1)Cr^{V}(HO^-)_2$, 136537-02-5; Pt, 7440-06-4; carbon, 7440-44-0.

Contribution from The Environmental Science Institute of Hyogo Prefecture, Yukihira-cho, Suma-ku, Kobe 654, Japan, Department of BioEngineering, Nagaoka University of Technology, Nagaoka 940-21, Japan, and Department of Synthetic Chemistry, Faculty of Engineering, Kyoto University, Kyoto 606, Japan

Iron(III) Porphyrins Substituted with Highly Electron-Withdrawing CF_3 Groups: Electronic Absorption, MCD, and EPR Spectral Study

Tetsuhiko Yoshimura,*[1a] Hiroo Toi,[1b] Shinji Inaba,[1b] and Hisanobu Ogoshi[1c]

Received October 9, 1990

Electronic absorption, MCD, and EPR spectra of iron(III) complexes of etioporphyrin I and electron-deficient porphyrins with one, two, or four CF_3 groups at pyrrole β-positions of the porphyrin have been measured. The overall equilibrium constants of the reaction of the iron(III) porphyrin chloride with imidazole and 1-methylimidazole were evaluated from the electronic spectral changes on addition of the bases. The equilibrium constants for imidazole have a slight tendency to decrease with the number of CF_3 group, and those for 1-methylimidazole have a marked such tendency. The effects of highly electron-withdrawing substituents at the porphyrin periphery were revealed more obviously in the MCD spectra of the (porphyrinato)iron(III) chloride than in the electronic spectra. MCD spectral results indicated that the Soret region is sensitive to minor changes in the redox potential of the porphyrin. In the EPR spectra of both low-spin complexes with imidazole and 1-methylimidazole, the g anisotropy was apparently lowered and the tetragonality μ/λ was increased with an increase in the number of CF_3 groups. The rhombicity R/μ for CF_3-substituted porphyrin complexes was larger than that for the unsubstituted analogues. These EPR spectral results were discussed in relation to the electron-withdrawing ability of peripheral substituents.

Introduction

The introduction of highly electron-withdrawing groups at the periphery of a porphyrin can affect the redox property of the porphyrin ligand and its respective metalloporphyrins and its affinity for metal ions or axial ligands.[2-5]

Electron-deficient porphyrins with chemically inert CF_3 groups at pyrrole β-positions have been shown to have a considerably reduced affinity for metal ions, arising from significant reduction in the electron density on pyrrole nitrogens.[6-8] Paramagnetic ^{19}F NMR spectra of iron(III) porphyrins substituted with CF_3 groups and reconstituted metmyoglobin have been measured and the ^{19}F

* To whom correspondence should be addressed.

(1) (a) The Environmental Science Institute of Hyogo Prefecture. (b) Nagaoka University of Technology. (c) Kyoto University.
(2) Falk, J. E. *Porphyrins and Metalloporphyrins*; Elsevier: Amsterdam, 1964.
(3) Caughey, W. S. In *Inorganic Biochemistry*; Eichhorn, G. L., Ed.; Elsevier: Amsterdam, 1973; Vol. 2, Chapter 24.
(4) Kadish, K. M. In *Iron Porphyrins*; Lever, A. B. P., Gray, H. B., Eds.; Addison-Wesley: Reading, MA, 1983; Part II, pp 161–249.
(5) Worthington, O.; Hambright, P.; Williams, R. F. X.; Reid, J.; Burnham, C.; Shamim, A.; Turay, J.; Bell, D. M.; Kirkland, R.; Little, R. G.; Datta-Gupta, N.; Eisner, U. *J. Inorg. Biochem.* **1980**, *12*, 281–291.

0020-1669/91/1330-4315$02.50/0 © 1991 American Chemical Society

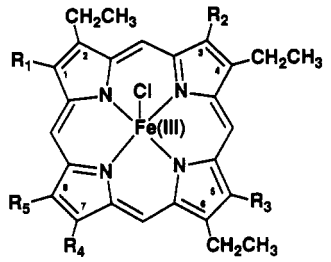

Figure 1. Structures of the iron(III) porphyrin chlorides studied: EtPI, $R_1 = R_2 = R_3 = R_4 = CH_3$, $R_5 = C_2H_5$; MTFP, $R_1 = CF_3$, $R_2 = R_3 = R_4 = R_5 = C_2H_5$; BTFP, $R_1 = R_5 = CF_3$, $R_2 = R_3 = R_4 = C_2H_5$; TTFP, $R_1 = R_2 = R_3 = R_4 = CF_3$, $R_5 = C_2H_5$.

Scheme I

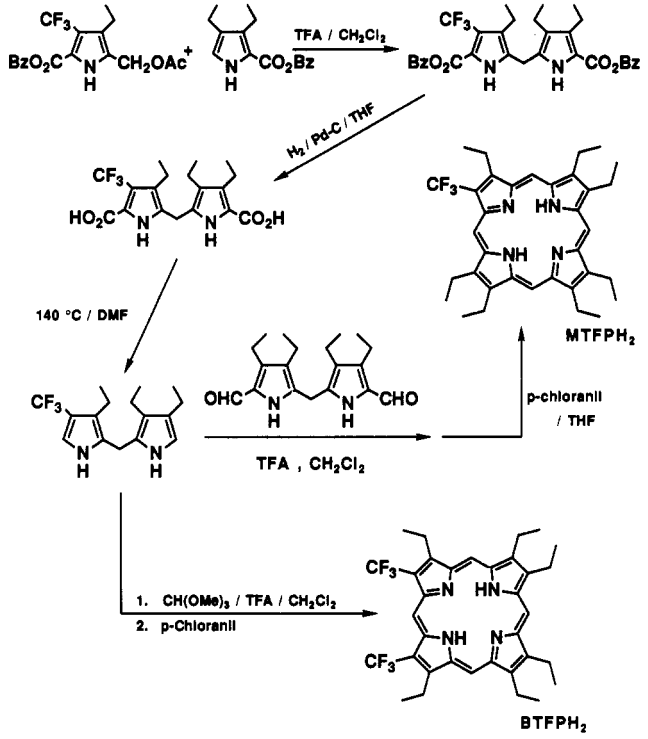

chemical shifts correlated to the spin states of the prosthetic group.[7,9] Recently, it has been reported that the introduction of electron-withdrawing groups to pyrrole β-positions of a porphyrin makes the metalloporphyrins resistant to oxidative degradation of the skeleton by strong oxidizing reagents, and its metalloporphyrins are available as good catalysts for benzene hydroxylation or as model complexes for cytochrome P-450.[10,11]

The transmission of electronic effects of the electron-withdrawing substituents on the porphyrin periphery can be expected to result in a considerable change in the spectral properties of the metalloporphyrin complexes.[2,3] In this study we describe the EPR, electronic absorption, and MCD spectral properties of iron(III) complexes of electron-deficient porphyrins with one, two, or four CF_3 groups at pyrrole β-positions of the porphyrin, which are the $(CF_3)_1$ derivative (its dianion, MTFP), the $(CF_3)_2$ derivative (its dianion, BTFP), and the $(CF_3)_4$ derivative (its dianion, TTFP), respectively, and compare their spectral properties with those of (etioporphyrinato I)iron(III) complexes (dianion of etioporphyrin I, EtPI) (Figure 1).

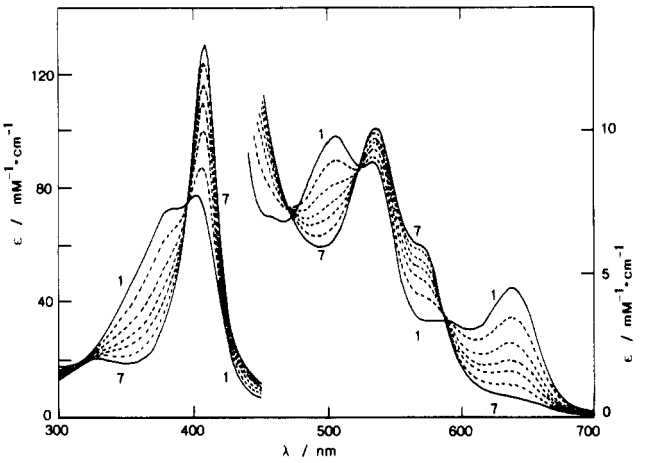

Figure 2. Spectral changes observed upon addition of imidazole (0–2.9 mM) to 0.017 mM solution of Fe(BTFP)Cl in chloroform. Imidazole concentrations: 1, 0 mM; 2, 0.4, mM; 3, 0.7, mM; 4, 1.0 mM; 5, 1.3 mM; 6, 1.8 mM; 7, 2.9 mM.

Experimental Section

Materials. Fe(EtPI)Cl was obtained commercially and Fe(TTFP)Cl was synthesized as described before.[6] $MTFPH_2$[12] and $BTFPH_2$[13] were synthesized from benzyl 5-(acetoxymethyl)-4-ethyl-3-(trifluoromethyl)-pyrrole-2-carboxylate as shown in Scheme I.[6] Chloroiron(III) complexes of MTFP and BTFP were prepared in the usual manner.[2,14] Imidazole (ImH) was recrystallized from chloroform–petroleum ether and 1-methylimidazole (*N*-MeIm) was stored over KOH and distilled by flowing N_2. All other chemicals used were obtained as the best available grade and were used without further purification.

Methods. The electronic absorption spectra were recorded on a Hitachi U-3210 spectrometer at 23 ± 1 °C. The MCD spectra were measured at room temperature with a JASCO J-500A spectropolarimeter attached to an electromagnet (1.3 T) and a JASCO DP-501 data processor for data accumulation and manipulation.

EPR measurements were carried out on a JEOL ME-3X spectrometer with 100-kHz field modulation. For accurate measurements of the EPR parameters, the microwave frequencies were measured with a digital frequency counter (Advantest, Model TR-5211A) and the magnetic field was calibrated with an NMR field meter (Echo Electronics, EMF 2000A). Since Fe(III)–BTFP and Fe(III)–TTFP complexes with *N*-MeIm are readily autoreduced to the Fe(II) derivatives, EPR spectra of the Fe(III) complexes were measured at 77 K immediately after the sample preparation.

The redox potentials ($E_{1/2}$) were calculated as the midpoints of the anodic and cathodic peak potentials of each redox couple in the cyclic voltammogram. Cyclic voltammetry under an argon atmosphere was monitored on a Yanaco P-1100 polarographic analyzer with a three-electrode system equipped with a Ag/AgCl reference electrode (BAS RE-1) and platinum electrodes at ambient temperature. The samples were dissolved in dry CH_2Cl_2 containing 0.1 M tetrabutylammonium perchlorate.

(6) Homma, M.; Aoyagi, K.; Aoyama, Y.; Ogoshi, H. *Tetrahedron Lett.* **1983**, *24*, 4343–4346.
(7) Toi, H.; Homma, M.; Suzuki, A.; Ogoshi, H. *J. Chem. Soc., Chem. Commun.* **1985**, 1791–1792.
(8) Aoyagi, K.; Toi, H.; Aoyama, Y.; Ogoshi, H. *Chem. Lett.* **1988**, 1891–1894.
(9) Abbreviations used: NMR, nuclear magnetic resonance; EPR, electron paramagnetic resonance; MCD, magnetic circular dichroism; MTFP, dianion of 1-(trifluoromethyl)-2,3,4,5,6,7,8-heptaethylporphyrin; BTFP, dianion of 1,8-bis(trifluoromethyl)-2,3,4,5,6,7-hexaethylporphyrin; TTFP, dianion of 1,3,5,7-tetrakis(trifluoromethyl)-2,4,6,8-tetraethylporphyrin; EtPI, dianion of etioporphyrin I or 1,3,5,7-tetramethyl-2,4,6,8-tetraethylporphyrin; OEP, dianion of octaethylporphyrin; PPIXDME, dianion of protoporphyrin IX dimethyl ester; P, dianion of porphyrin; ImH, imidazole; *N*-MeIm, 1-methylimidazole; Py, pyridine; B, base.
(10) Traylor, T. G.; Tsuchiya, S. *Inorg. Chem.* **1987**, *26*, 1338–1339.
(11) Tsuchiya, S.; Seno, M. *Chem. Lett.* **1989**, 263–266.
(12) ^1H NMR ($CDCl_3$): δ −3.74 (br, 2 H, N*H*), 1.90 (m, 21 H, $-CH_2CH_3$), 4.00, 4.14, 4.29 (m, 4 H, 8 H, and 2 H, respectively, $-CH_2CH_3$), 10.08, 10.22, 10.36 (s, 2 H, 1 H, respectively, meso-*H*). ^{19}F NMR (external $CFCl_3$, $CDCl_3$): δ −51.7 (s). Vis (CH_2Cl_2) [λ_{max}, nm (relative absorption intensity)]: 401 (1.00), 505 (0.0522), 542 (0.0655), 567 (0.0386), 621 (0.006). MS: *m/e* 574 (M^+), 573 ($M^+ - 1$).
(13) ^1H NMR ($CDCl_3$): δ −3.52 (br, 2 H, N*H*), 1.92 (m, 18 H, $-CH_2CH_3$), 4.04, 4.32 (m, 8 H and 4 H, respectively, $-CH_2CH_3$), 10.07, 10.15, 10.60 (s, 1 H, 2 H, and 1 H, respectively, meso-*H*). ^{19}F NMR (external $CFCl_3$, $CDCl_3$): δ −50.8 (s). Vis (CH_2Cl_2) [λ_{max}, nm (relative absorption intensity)]: 405 (1.00), 503 (0.0620), 537 (0.0336), 574 (0.0265), 627 (0.0211). MS: *m/e* 614 (M^+), 613 ($M^+ - 1$).
(14) Ogoshi, H.; Sugimoto, H. In *The Chemistry of Porphyrins*; Osa, T., Ed.; Kyoritsu Shuppan: Tokyo, 1982; p 40.

Table I. Equilibrium Constants for Addition of Imidazole and 1-Methylimidazole to the Chlorides of Iron(III) Etioporphyrin I and Iron(III) Porphyrins Substituted with CF_3 Groups[a]

porphyrin	$E_{1/2}^1$/V[b]	base	log β_2[c]
EtPI	−1.39	ImH	6.24 ± 0.02
MTFP	−1.22	ImH	6.18 ● 0.03
BTFP	−1.08	ImH	6.17 ± 0.02
TTFP	−0.81	ImH	6.15 ± 0.05
EtPI	−1.39	*N*-MeIm	3.67 ± 0.04
MTFP	−1.22	*N*-MeIm	3.25 ± 0.02

[a] Solvent, $CHCl_3$; temperature, 23 ± 1 °C. [b] The first redox potentials of the free-base porphyrins. [c] β_2 in units of M^{-2}.

Results and Discussion

Equilibria of Imidazole and 1-Methylimidazole with Iron(III) Porphyrins. The addition of imidazole to Fe(BTFP)Cl in chloroform resulted in the spectral changes in Figure 1. The spectra had isosbestic points at 396, 472, 523, and 588 nm. However, only the absorption line of Fe(BTFP)Cl (spectrum 1 in Figure 2) slightly deviated from the isosbestic points.

Upon the addition of imidazole or 1-methylimidazole to four different iron(III) porphyrin chlorides, the absorption intensities in wavelength ranges of 320–390, 470–520, and above 590 nm were decreased while those in wavelength ranges of 400–460 and 530–570 nm were increased. In these spectral changes, the isosbestic points were observed at positions similar to those of the Fe(BTFP)Cl–ImH system (Figure 2), though the absorption lines at low concentrations of bases often deviated from the isosbestic points. These overall spectral changes from high-spin-type to low-spin-type spectra are very similar to those upon addition of imidazole derivatives to (deuteroporphyrin IX dimethyl esterato)iron(III)[15] and (protoporphyrin IX dimethyl esterato)iron(III).[16]

The reaction of (porphyrinato)iron(III) chloride (FePCl) with nitrogenous bases (B) can proceed in two steps.

$$\mathrm{FePCl} + \mathrm{B} \overset{K_1}{\rightleftharpoons} \mathrm{FePBCl} \quad (1)$$

$$\mathrm{FePBCl} + \mathrm{B} \overset{K_2}{\rightleftharpoons} \mathrm{FePB_2Cl} \quad (2)$$

Since K_2 is much greater than K_1, the electronic spectrum of the intermediate species, FePBCl, is generally not observed,[16-18] though it has been observed in the system of FePCl with hindered imidazoles.[16] Thus, the reaction of unhindered bases such as imidazole and 1-methylimidazole proceeds apparently in one step.

$$\mathrm{FePCl} + 2\mathrm{B} \overset{\beta_2}{\rightleftharpoons} \mathrm{FePB_2Cl} \quad (3)$$

Accordingly, the deviation from the isosbestic points at the low concentrations of bases mentioned above is attributable to the formation of the intermediary mono(base) adduct FePBCl.

The overall equilibrium constants (β_2) were evaluated from the spectral changes on addition of imidazole and 1-methylimidazole to FePCl (P = EtPI, MTFP, BTFP, TTFP) in chloroform. If the concentration of a base, [B], is much larger than [FePCl], the following equation can be obtained from the equation of Miller and Dorough:[17,19,20]

$$\log (A - A_0)/(A_C - A) = \log \beta_2 + n \log [\mathrm{B}] \quad (4)$$

Here A is the observed absorbance at a given wavelength, A_0 is the absorbance of FePCl in the absence of base, A_C is the absorbance in the presence of a large excess of base, and n represents the coordination number. It is possible to evaluate log β_2 from the intercept of plots of log $(A - A_0)/(A_C - A)$ against log [B]

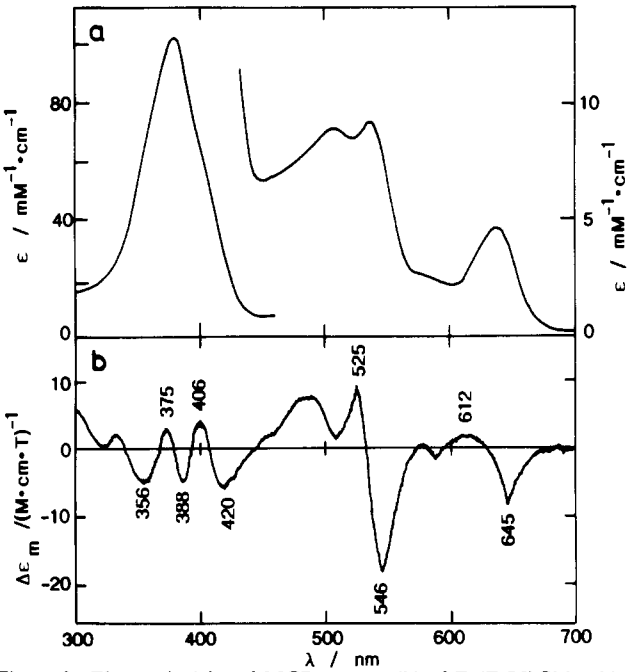

Figure 3. Electronic (a) and MCD spectra (b) of Fe(EtPI)Cl in chloroform at room temperature. [Fe(EtPI)Cl] = 0.0157 mM.

in which the slope (n) is 2.0. This linear plot was obtained from the data at five wavelengths, 370, 495, 570, and 639 nm, in the Fe(BTFP)Cl–ImH system (Figure 2); the data in the other systems were also taken at five similar wavelengths.

The mean values of log β_2 and the standard deviations are shown in Table I, together with the first redox potentials of the free-base porphyrins. As the number of CF_3 groups increases, the redox potential becomes more positive and thus the reduction of the porphyrin becomes easier. In the metalloporphyrins, the increase in electron-withdrawing ability of porphyrin peripheral substituents results in a decrease in electron density on the pyrrole nitrogen. Concomitantly, the affinity of metal ion for axial ligands increases in the metalloporphyrins of Co(II),[21] Ni(II),[22] and V(IV),[22] while it decreases in iron(III) porphyrins because of destabilization of the positive charge on Fe(III).[17]

As shown in Table I, the equilibrium constants for imidazole have a slight tendency to decrease with the number of CF_3 groups. The tendency is more marked for 1-methylimidazole. (The equilibrium constants with 1-methylimidazole for Fe(III)–BTFP and Fe(III)–TTFP cannot be evaluated because Fe(III) is reduced to Fe(II) in these systems. The redox potentials of BTFP and TTFP (Table I) shift markedly to anodic direction, and so Fe(III) in their complexes is readily autoreduced to Fe(II) by 1-methylimidazole as well as pyridine[23] and piperidine.[24])

It has been demonstrated by Walker et al. that the stabilization by the delocalization of the positive charge on Fe(III) through hydrogen bonding of the NH group in NH imidazoles (e.g., imidazole and 4-methylimidazole) makes the log β_2 values for NH imidazoles to be larger than those for NR imidazoles (e.g., 1-methylimidazole) by about 3 log units.[17] The magnitude of this stabilization effect in log β_2 values for NH imidazoles is found to differ for each porphyrin ligand. The difference in log unit between log β_2 for imidazole and for 1-methylimidazole is 3.0 for TPP,[17] 2.2 for OEP,[17] 3.0 for PPIXDME,[16] 2.6 for EtPI, and 2.9 for MTFP. Thus, there is a tendency for the difference to increase as the redox potentials of free-base porphyrin become more positive or as the electron-withdrawing ability of the peripheral substituents

(15) Momenteau, M. *Biochim. Biophys. Acta* **1973**, *304*, 814–827.
(16) Yoshimura, T.; Ozaki, T. *Bull. Chem. Soc. Jpn.* **1979**, *52*, 2268–2275.
(17) Walker, F. A.; Lo, M.-W.; Ree, M. T. *J. Am. Chem. Soc.* **1976**, *98*, 5552–5560.
(18) Balke, V. L.; Walker, F. A.; West, J. T. *J. Am. Chem. Soc.* **1985**, *107*, 1226–1233.
(19) Miller, J. R.; Dorough, G. D. *J. Am. Chem. Soc.* **1952**, *74*, 3977–3981.
(20) Tsuchida, E.; Honda, K.; Hasegawa, E. *Biochim. Biophys. Acta* **1975**, *393*, 483–495.
(21) Walker, F. A.; Beroiz, D.; Kadish, K. M. *J. Am. Chem. Soc.* **1976**, *98*, 3484–3489.
(22) Walker, F. A.; Hui, E.; Walker, J. M. *J. Am. Chem. Soc.* **1975**, *97*, 2390–2397.
(23) Weightman, J. A.; Hoyle, N. J.; Williams, R. J. P. *Biochim. Biophys. Acta* **1971**, *244*, 567–572.
(24) Gaudio, J. D.; La Mar, G. N. *J. Am. Chem. Soc.* **1978**, *100*, 1112–1119.

Table II. Electronic Spectral Data for Iron(III) Porphyrin Chlorides and their Complexes with N-Bases[a]

porphyrin	base	abs max/nm (ϵ/mM^{-1} cm^{-1})			
		Soret	visible		
EtPI	none	378.8 (100)	508.8 (8.8)	535.2 (9.2)	637.6 (4.6)
	ImH	404.4 (146)	528.0 (10.3)	556 sh (8.0)	
	N-MeIm	404.0 (151)	525.6 (11.0)	551 sh (8.9)	
	Py	398.8 (141)	520.0 (10.9)	551 sh (8.7)	
MTFP	none	383.6 (91.0)	505.2 (9.8)	537.2 (9.8)	636.0 (4.3)
	ImH	406.4 (152)	531.2 (11.0)	566.0 (8.1)	
	N-MeIm	406.0 (156)	529.2 (11.3)	564.4 (8.5)	
	Py	402.0 (130)	526.4 (10.8)	555.6 (9.0)	
BTFP	none	401.6 (80.1)	505.2 (10.1)	534.4 (9.3)	637.6 (4.7)
	ImH	408.4 (144)	536.0 (10.8)	570 sh (6.6)	
	N-MeIm[d,e]	409.2 (137)	530.0 (10.7)	557.2 (8.4)	
	Py[e]	405.2 (106)	525.2 (9.3)	544.0 (8.6)	554.8 (9.4)
TTFP[f]	none	407.6 (91.5)	506.4 (9.5)	533.6 (9.5)	633.6 (4.0)
	ImH	410.8 (137)	540.0 (10.2)	572 sh (5.0)	

[a] Solvent, $CHCl_3$; temperature, 23 ± 1 °C. sh = shoulder. [b] [FePCl] = 0.013–0.018 mM. [c] [ImH] = 0.23 M, [*N*-MeIm] = 2.4 M, and [Py] = 4.0 M, unless otherwise stated. [d] [*N*-MeIm] = 3.6 M. [e] A small portion of Fe(III) was autoreduced to Fe(II) on the addition of the base. [f] In the complexes with 1-methylimidazole and pyridine, a large portion of Fe(III) was autoreduced to Fe(II) on the addition of the base and so those data were not shown in the table.

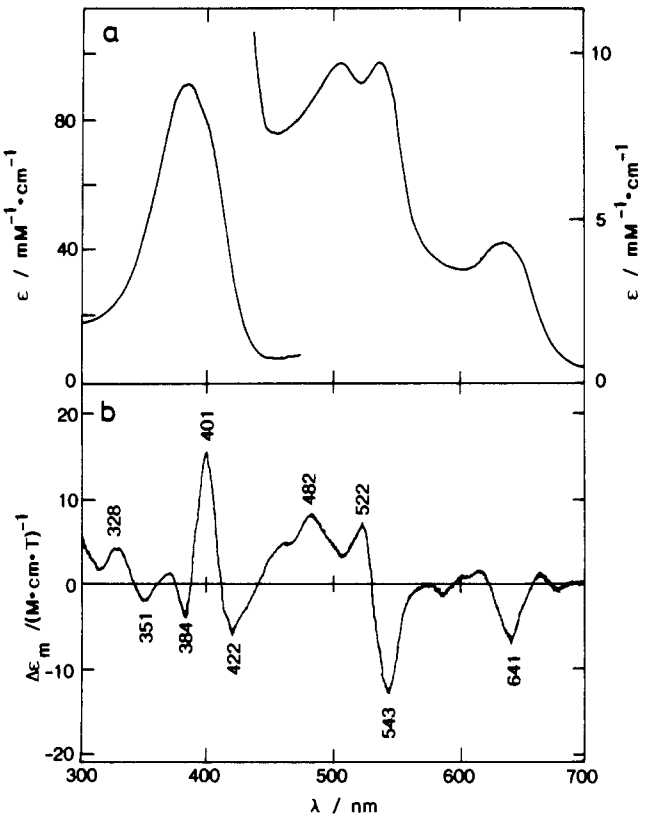

Figure 4. Electronic (a) and MCD spectra (b) of Fe(MTFP)Cl in chloroform at room temperature. [Fe(MTFP)Cl] = 0.0131 mM.

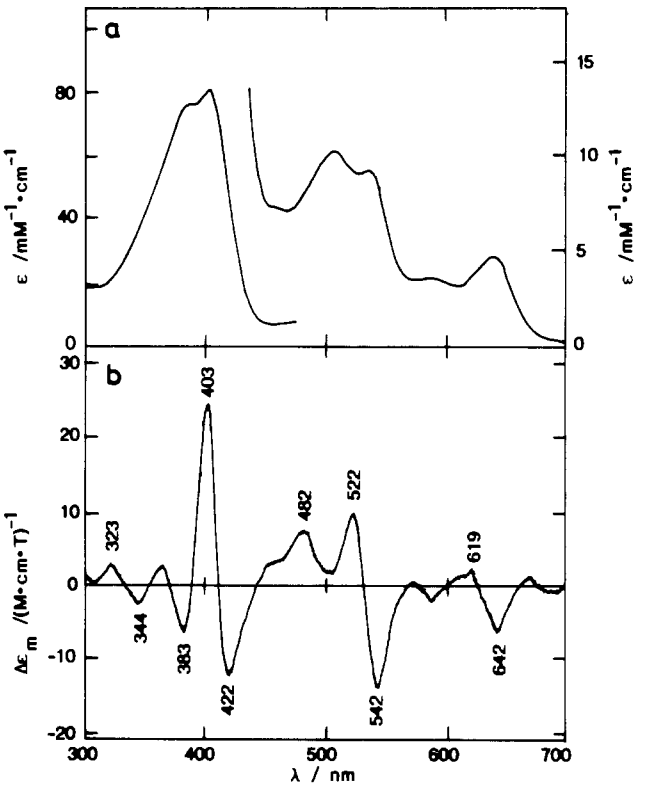

Figure 5. Electronic (a) and MCD spectra (b) of Fe(BTFP)Cl in chloroform at room temperature. [Fe(BTFP)Cl] = 0.0179 mM.

increases. This also suggests that the electron-withdrawing substituents cause the positive charge on Fe(III) to destabilize.

Electronic and MCD Spectra. Figures 3–6 show electronic absorption and MCD spectra of iron(III) porphyrin chlorides, and Figures 7 and 8 show those of iron(III) porphyrin complexes with imidazole in chloroform in the wavelength region from 300 to 700 nm. The electronic absorption spectral data for iron(III) porphyrin chlorides and their complexes with imidazole, 1-methylimidazole, and pyridine are listed in Table II.

The overall absorption spectral patterns of iron(III) porphyrin chloride and its complexes with N-bases are similar to those of Fe(III) complexes of meso-unsubstituted porphyrins such as octaethylporphyrin,[25,26] deuteroporphyrin IX dimethyl ester,[15] and protoporphyrin IX dimethyl ester.[16] As shown in Table II, the Soret band of both chloride and bis(adduct) with N-bases is found to be shifted to longer wavelengths as the redox potential of the porphyrin becomes more positive, although the visible absorption bands are apparently independent of the redox potential in wavelength. The Soret and visible absorption maxima for substituted metal deuteroporphyrin complexes have been also shown to be shifted to longer wavelengths with decrease in porphyrin basicity (pK_3 value).[2,3] Thus, the highly electron-withdrawing substituents at the porphyrin periphery induce shifts to longer wavelengths in absorption maxima of meso-unsubstituted porphyrins and the metalloporphyrins.

MCD spectral band positions, patterns, and intensities for the five-coordinated high-spin iron(III) porphyrin complexes as well

(25) Ogoshi, H.; Sugimoto, H.; Yoshida, Z. *Biochim. Biophys. Acta* **1980**, *621*, 19–28.

(26) Kobayashi, H.; Higuchi, T.; Eguchi, K. *Bull. Chem. Soc. Jpn.* **1976**, *49*, 457–463.

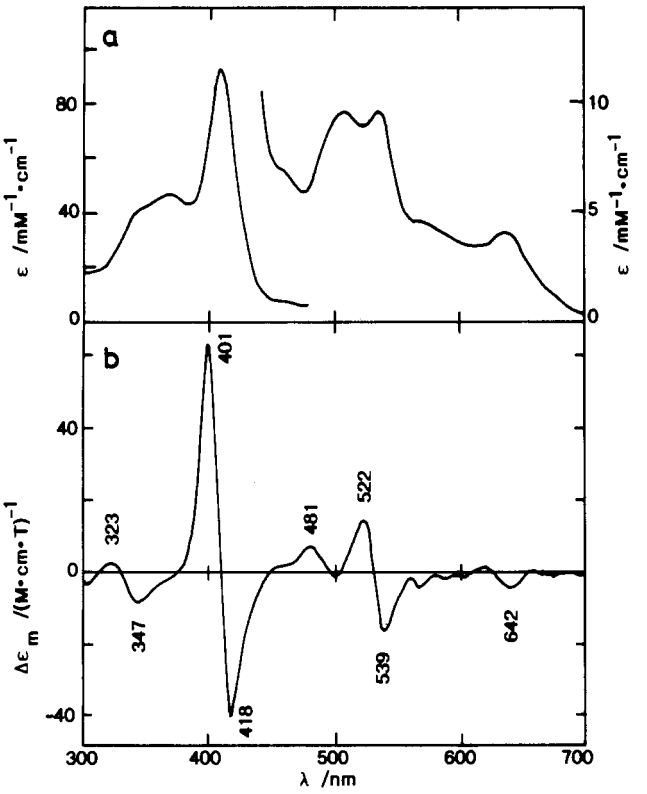

Figure 6. Electronic (a) and MCD spectra (b) of Fe(TTFP)Cl in chloroform at room temperature. [Fe(TTFP)Cl] = 0.0167 mM.

as the iron(III) hemoproteins have been demonstrated to be sensitive to the nature of axial ligand and the polarity of solvent.[26-31] The MCD spectral band patterns of four iron(III) porphyrin chlorides (Figures 3–6) which are in the high-spin state apparently resemble each other in the visible Q-band region, while they are markedly different in the Soret band region. The MCD spectrum in the visible Q-band region is composed of an apparent Faraday *A* term coupled with a *B* term.[26] The derivative-shaped MCD band with a peak around 400 nm and a trough around 420 nm is intensified with an increase in the number of CF_3 group on the porphyrin periphery, accompanying the relative decrease in the intensity of the trough around 385 nm in Fe(MTFP)Cl and Fe(BTFP)Cl and the disappearance of the band in Fe(TTFP)Cl. Concomitantly, in the electronic spectra the intensity of absorption around 405 nm gradually increases and the shape varies from shoulder to hump and to single peak; the reverse is found for the absorption around 380 nm. These results suggest that the Soret absorption band of iron(III) porphyrin chloride with weak electron-withdrawing substituents is dominantly characterized by the absorption band around 380 nm which exhibits a weak MCD signal and that of the chloride with strong electron-withdrawing substituents is characterized by the absorption band around 405 nm which exhibits a intense MCD signal. Thus, as the electron-withdrawing ability of the substituents rises, the contribution of the 405-nm band to the Soret absorption band becomes greater than that of 380-nm band. Consequently, the Soret band in the electronic spectrum can be shifted to longer wavelengths and the MCD band can be intensified.

Figure 9 illustrates the plots of MCD intensities of a peak around 400 nm (406–401 nm), a trough around 540 nm (546–539 nm), and a trough around 645 nm (645–641 nm) against the redox potential of each porphyrin. As shown in Figure 9, the MCD intensity of the peak around 400 nm markedly varies with the redox potential of the porphyrin, while the intensities of troughs around 540 and 645 nm only slightly do. This indicates the MCD band in the Soret region of iron(III) porphyrin chlorides is sensitive to minor changes in the redox potential of the porphyrin or the electron-withdrawing or -donating ability of the porphyrin substituents.

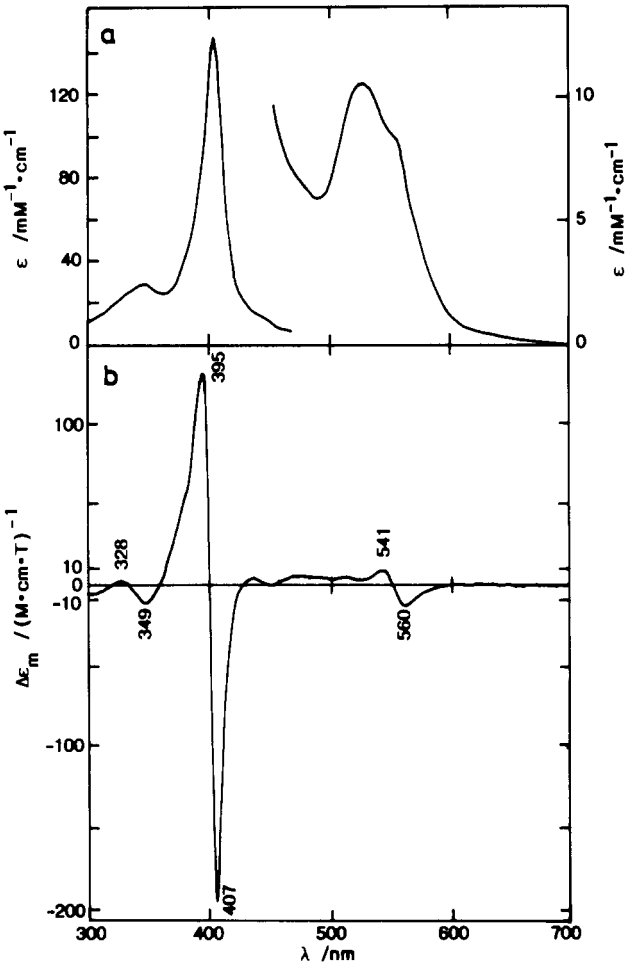

Figure 7. Electronic (a) and MCD spectra (b) of the Fe(EtPI)Cl–ImH system in chloroform at room temperature. [Fe(EtPI)Cl] = 0.0157 mM: [ImH] = 15 mM.

The MCD spectral patterns of low-spin iron(III) porphyrin complexes with imidazole (Figures 7 and 8) are similar to those of iron(III) hemoprotein analogues, in which the MCD bands for the Soret and visible regions are composed predominantly of Faraday *C* terms and of *A* terms, respectively.[26] In the MCD as well as the electronic spectra, the bands for the Fe(EtPI)Cl–ImH system appeared at shorter wavelengths than those for the Fe(TTFP)Cl–ImH system.

It therefore appears that the MCD spectra of iron(III) porphyrin complexes, as well as those of bis(imidazole)iron(II) porphyrin systems,[32] are sensitive to the porphyrin peripheral substituents.

EPR Spectra. EPR spectra of the complexes were measured in chloroform at 77 K. Four iron(III) porphyrin chlorides and their complexes with imidazole and 1-methylimidazole exhibited the high-spin spectrum with $g_\perp = 6.1$ and $g_\parallel = 2.0$ and the low-spin spectrum with three *g* values, respectively. The low-spin *g* values and the crystal field parameters (μ/λ and R/μ) obtained by Bohan's method[33] are listed in Table III, where λ is a spin–orbit coupling constant. The two crystal field parameters, rhombicity (R/μ) and tetragonality (μ/λ), which can be calculated from the

(27) Hatano, M.; Nozawa, T. *Adv. Biophys.* **1978**, *11*, 95–149.
(28) Nozawa, T.; Ookubo, S.; Hatano, M. *J. Inorg. Biochem.* **1980**, *12*, 253–267.
(29) Ookubo, S.; Nozawa, T.; Hatano, M. *J. Inorg. Biochem.* **1989**, *35*, 305–317.
(30) Vickery, L.; Nozawa, T.; Sauer, K. *J. Am. Chem. Soc.* **1976**, *98*, 343–350.
(31) Dawson, J. H.; Dooly, D. M. In *Iron Porphyrins*; Lever, A. B. P., Gray, H. B., Eds; Addison-Wesley: Reading, MA, 1989; Part III, pp 1–135.
(32) Svastits, E. W.; Dawson, J. H. *Inorg. Chim. Acta* **1986**, *123*, 83–86.
(33) Bohan, T. L. *J. Magn. Reson.* **1977**, *26*, 109–118.

Table III. EPR Parameters of Low-Spin Bis(N-Base) Complexes of Iron(III) Etioporphyrin I and Iron(III) Porphyrins Substituted with CF_3 Groups

porphyrin	$E_{1/2}^{I}$/V[a]	base	g values			cryst field params		normalization factor[b]
			g_1	g_2	g_3	μ/λ	R/μ	
ETPI	−1.39	ImH	2.941	2.257	1.511	3.30	0.567	1.004
MTFP	−1.22	ImH	2.871	2.299	1.612	3.42	0.625	1.010
BTFP	−1.08	ImH	2.830	2.299	1.641	3.49	0.645	1.009
TTFP	−0.81	ImH	2.812	2.300	1.670	3.62	0.647	1.011
ETPI	−1.39	*N*-MeIm	2.937	2.265	1.506	3.22	0.581	1.004
MTFP	−1.22	*N*-MeIm	2.843	2.307	1.594	3.22	0.670	1.005
BTFP	−1.08	*N*-MeIm	2.822	2.303	1.617	3.32	0.672	1.004
TTFP	−0.81	*N*-MeIm	2.806	2.306	1.655	3.47	0.671	1.008

[a] See footnote *b* of Table I. [b] Calculated from the coefficients of the ground doublet.

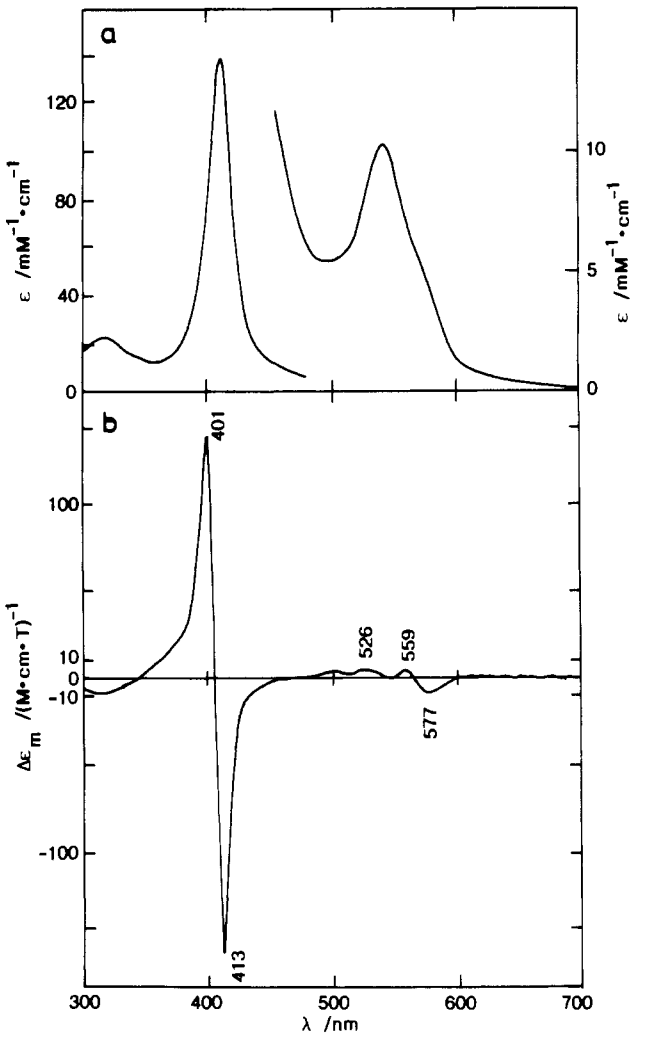

Figure 8. Electronic (a) and MCD spectra (b) of the Fe(TTFP)Cl–ImH system in chloroform at room temperature. [Fe(TTFP)Cl] = 0.0167 mM; [ImH] = 15 mM.

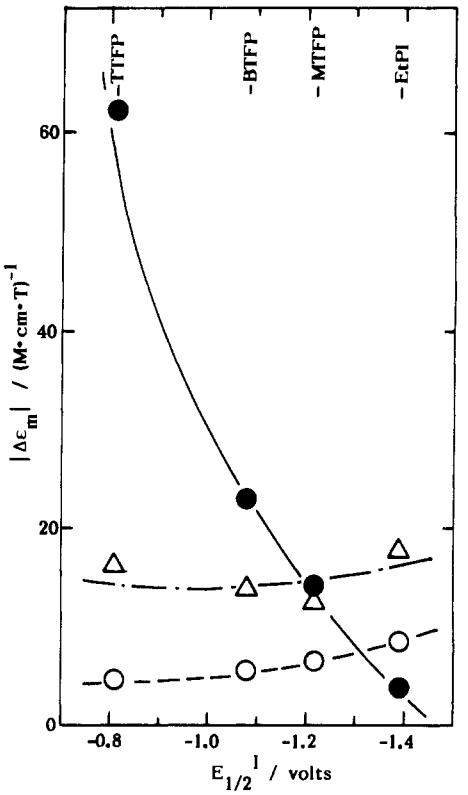

Figure 9. Plots of MCD intensities (absolute values) of a peak around 400 nm (●), a trough around 540 nm (△), and a trough around 645 nm (○) in the MCD spectra of iron(III) porphyrin chlorides against the redox potential of each porphyrin.

low-spin g values,[33-37] are a purely geometric factor and a measure of the total electron donation by the axial ligand in the heme coordination sphere, respectively.[37,38] These parameters have been utilized by many investigators to identify the two axial ligands of low-spin iron(III) hemoproteins and iron(III) porphyrin complexes.[34,37-42] In Bohan's method, attention is given to the signs of the g values and to the assignment of three measured g values to the respective Cartesian axes, and when the crystal field parameters are calculated from the g values with different arrangements which correspond to different coordinate systems and they satisfy the conditions of a minimum value for $|R/\mu|$ or $|R/\mu| \leq {}^2/_3$ and a positive value for R, its coordinate system is defined to be "proper". In this study, the sign and the assignment of the g values employed in the parameter calculation were assumed to be identical [e.g., $(g_x, g_y, g_z) = (-2.257, -1.511, 2.941)$ for Bohan convention III] in order to compare the parameters of the eight complexes, though the R/μ values for three CF_3-substituted porphyrin complexes with 1-methylimidazole in Table III exceed ${}^2/_3$.

As shown in Table III, the g anisotropy in both low-spin complexes with imidazole and 1-methylimidazole is apparently lowered with an increase in the number of a CF_3 groups on the porphyrin

(34) Palmer, G. In *Iron Porphyrins*; Lever, A. B. P., Gray, H. B., Eds.; Addison-Wesley: Reading, MA, 1983; Part II, pp 43–88.
(35) Griffith, J. S. *Nature (London)* **1957**, *180*, 30–31.
(36) Kotani, M. *Adv. Chem. Phys.* **1964**, *7*, 159–181.
(37) Blumberg, W. E.; Peisach, J. In *Bioinorganic Chemistry*; Gould, R. F., Ed.; American Chemical Society: Washington, DC, 1971; p 271.
(38) Peisach, J.; Blumberg, W. E.; Adler, A. *Ann. N.Y. Acad. Sci.* **1973**, *206*, 310–327.
(39) Quinn, R.; Nappa, M.; Valentine, J. S. *J. Am. Chem. Soc.* **1982**, *104*, 2588–2595.
(40) Yoshimura, T.; Ozaki, T. *Arch. Biochem. Biophys.* **1984**, *230*, 466–482.
(41) Walker, F. A.; Reis, D.; Balke, V. L. *J. Am. Chem. Soc.* **1984**, *106*, 6888–6898.
(42) Sakurai, H.; Yoshimura, T. *J. Inorg. Biochem.* **1985**, *24*, 75–96.

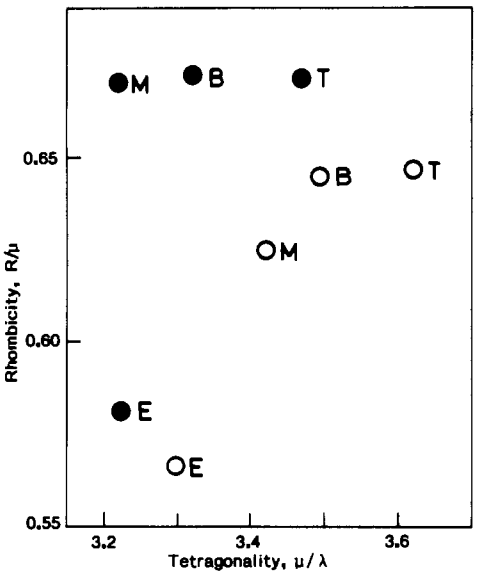

Figure 10. Crystal field diagram for iron(III) porphyrin complexes with imidazole (O) and 1-methylimidazole (●). E, M, B, and T represent the EtPI, MTFP, BTFP, and TTFP complexes, respectively.

periphery. As illustrated in Figure 10, the values of μ/λ appear to increase with an increase in the CF_3 number. In iron(III) porphyrin bis(imidazole) complexes and iron(III) hemoprotein complexes with bis(imidazole) (or bis(histidine)) which show low-spin EPR spectra, the g anisotropy has been reported to be lowered and the μ/λ values to be increased when the coordinated imidazole is linked by a hydrogen bond to free imidazole, anionic groups, or amino acid residues, and it is deprotonated to form an imidazolate anion.[37-41] These results were discussed in relation to an increase in basicity or σ-electron-donor ability of coordinated imidazole(s), which is induced from the partial or complete ionization of pyrrole-type hydrogen. In the systems studied here, the σ-electron donation from the axial imidazole to iron can be enhanced by the introduction of the highly electron-withdrawing CF_3 groups to the porphyrin periphery, which may lead to an increase in the μ/λ values.

The R/λ values for CF_3-substituted porphyrin complexes are distinguished from those for the unsubstituted etioporphyrin complexes and are found to be appreciably large, since the value is defined to be less than or equal to $^2/_3$.[33,37] This suggests that some distortion in the porphyrinato plane results from the introduction of highly electron-withdrawing CF_3 groups.

As described above, the equilibrium constants for the reaction of iron(III) porphyrins with imidazole derivatives are profoundly dependent upon whether the derivatives have a dissociable proton or not. Such a difference in chemical structure of the imidazole derivatives affects the crystal field parameters of the iron(III) porphyrin complexes. As shown in Figure 10, tetragonality μ/λ values of imidazole complexes can be slightly larger than those of 1-methylimidazole complexes with analogous porphyrinato ligand, while for the rhombicity R/μ the relation is reversed. The difference in crystal field parameters between imidazole and 1-methylimidazole complexes can be elucidated as follows. In the complexes with imidazole containing a dissociable proton, the electron deficiency derived from the substitution of highly electron-withdrawing groups at the porphyrin periphery is transmitted to the axial imidazoles and ionizes to some extent the N_1 proton of imidazole to donate the negative charge to iron; consequently, the iron(III) complexes are stabilized. On the other hand, in the complexes with 1-methylimidazole, the absence a dissociable proton precludes this stabilizing effect and thus the geometric alteration in heme stereochemistry may be somewhat more intensely induced by perturbation from the electron deficiency than that for imidazole complexes.

Acknowledgment. We wish to express our gratitude to Dr. S. Suzuki of the College of General Education, Osaka University, for measurement of MCD spectra and for helpful discussions. This research was supported in part by a grant from the Yamagata Technopolis Foundation.

Registry No. Fe(EtPI)Cl-ImH, 136184-95-7; Fe(MTFP)Cl-ImH, 136213-09-7; Fe(BTFP)Cl-ImH, 136184-96-8; Fe(TTFP)Cl-ImH, 136184-97-9; Fe(EtPI)Cl-*N*-MeIm, 76581-43-6; Fe(MTFP)Cl-*N*-MeIm, 136155-39-0.